

## Challenges of the Seismic Image Resolution for Gas Exploration in the East Mediterranean Sea

Barakat, M. Kh. <sup>a\*</sup>, El-Gendy, N. <sup>a</sup>, El-Nikhely, A. <sup>b</sup>, Zakaria, A. <sup>c</sup>, and Hellish, H. <sup>d</sup>

<sup>a</sup> Geology Department, Faculty of Science, Tanta University, Tanta 31527, Egypt

<sup>b</sup> Physics Department, Faculty of Science, Alexandria University, Alexandria, Egypt

<sup>c</sup> Seismic data processing consultant, Dana petroleum

<sup>d</sup> Project Geophysicist at Petroleum Geo-Service (PGS)

\*Corresponding author: [moatazbarakat@science.tanta.edu.eg](mailto:moatazbarakat@science.tanta.edu.eg)  
[moatazbarakat@yahoo.com](mailto:moatazbarakat@yahoo.com)

### Abstract

Some discoveries in the East Mediterranean have been made in recent years, and production has begun. In 2015, the most promising exploration was the Zohr field off-shore Egypt. Many 2D/3D marine seismic acquisition surveys were conducted using improved technology to obtain a higher resolution image of the subsurface Mediterranean. Optimal acquisition and processing parameterization are required to obtain higher resolution subsurface images.

The work includes a summary of the most interesting basins in the East Mediterranean in terms of geology and structure, as well as the challenges of seismic exploration and a workflow to eliminate one of the most prevalent phenomena in marine seismic acquisition which known by bubbles effect.

The bubble energy causes the appearance of low-frequency periodic events following all refractors, resulting in poor seismic image resolution. The application of wavelet-dependent De-signature workflow will be discussed in this work, over the study area from offshore Egypt, which is characterised by a complex water bottom.

The proposed workflow shows a good and stable result in attenuating the bubble energy. It is now possible to completely remove the bubble effect from data using robust and consistent acquisition parameters, in addition to the application of the presented optimum proposed workflow.

### Article Info

Received 19 Jul. 2021

Revised 7 Sep. 2021

Accepted 18 Sep. 2021

### Keywords

Seismic Processing; De-signature filter; Wiener filter; bubble effect; Mediterranean Sea; and Egypt.

### Introduction

The offshore East Mediterranean region plays important role in oil and gas field. It has received increased international interest in the last few years, especially after recent huge reservoirs of gas have been discovered in offshore Egypt and Cyprus.

Based on the recent discoveries, The East Mediterranean is the hottest spot area for exploration compared with the West Mediterranean. The discovery of the Zohr field in the Levantine basin, offshore Egypt in 2015 changes the game of exploration in the Mediterranean Sea. Many international companies are now looking for new discoveries in the region. Therefore, updating

subsurface seismic images are required to get clear information for the interesting areas. Recently, many activities of new 2D/3D seismic acquisition surveys are acquired looking for a high-resolution subsurface image using recently high technology in the marine acquisition and processing.

The resolution of the seismic images is the most important step for any exploration to identify the subsurface structure. Seismic imaging resolution is always challenging and depends on many factors:

- The complexity of subsurface geology (structure and lithology).
- The target levels (shallow or deep).

- The type of the acquisition survey 2D/3D.
- The Optimum seismic processing flows.

The complex geological setting of the East Mediterranean Sea shows shallow carbonate reefs and shallow canyons which generate several multiple diffractions and undesired signal. The recording of the complexity of the seafloor is contaminated with complex seismic response need more effort to remove the undesired recorded response. Removing the source signature generation in the seismic acquisition is considered as one of the main challenges in the complex areas to get broadband seismic data processing and aim to get true earth response (Belhassen et al., 2017) [1].

The bubble energy removal and zero phasing of marine seismic data are known as the De-signature process and usually applied using a deterministic inverse filter. They are used to eliminate the bubble effect from the recorded seismic data. Most of these techniques depend on the two wavelets, the first wavelet is the recorded or modelled Far-Field signature and the second one is the desired output. Other techniques apply predictive deconvolution to remove the reverberation of the bubbles (Egbai et al., 2012) [2]. The stability of the source parameter in the seismic acquisition plays an important role in modelling and recording stable Far-Field signatures, which can be used as a reference input wavelet to the De-signature stage, especially in the case of dual and triple sources acquisition. The consistency of the source parametrizations in terms of air gun pressure, volume, source depth, array separation, and vessel speed improve the overall performance of the De-signature process.

## Geological Setting

The Eastern Mediterranean is separated from the Western one by the Sicily channel and characterized by different ages and settings. The Eastern Mediterranean is the oldest and deepest point portion of the oceanic lithosphere mainly pre-Jurassic to Cretaceous age that is subducting under the Eurasian plate. The Western Mediterranean is much younger to the Eastern. It was developed as the now consumed oceanic crust of the African plate (the so-called Neo-Tethys, or Alpine Tethys) was subducted under Eurasia. (S. Goffredo and Z. Dubinsky 2014), [3].

The East Mediterranean was originated due to several phases of rifting between the major plates of Africa and Eurasia during the Early Triassic–Late Cretaceous (Gradmann et al., 2005) [4], The bedrock is of Triassic age and has proved to be of highly attenuated continental crust origin (Ben-Avraham et al., 2002) [5].

The East Mediterranean includes two major basins of nearly the same age, the Levantine, and the Herodotus (Fig. 1). They have the same sediment type with the same thicknesses (10-15 km), but the Herodotus basin is approximate twice the size of the Levantine basin. Structural and stratigraphic (anticlines, pinch-outs, unconformities) traps are mainly common for both basins. The cap-rock for the Levantine basin includes Messinian evaporites, Triassic, Jurassic and Cretaceous clays and marls,

Triassic and Jurassic evaporites. However, the cap-rock for Herodotus includes Messinian evaporites, calcareous siltstone slower-middle Miocene, and siltstones of Pleistocene due to the Nile cone sediment. The Levant Basin contains more than 14 km of Mesozoic–Cenozoic successions, including up to 2 km of Messinian salt, The Herodotus basin contains more than 7 km of Mesozoic–Cenozoic successions (Voogd and Truffert, 1992 [6]; Garfunkel, 1998) [7], which is overlain by up to 2–3 km of Messinian salt (Barakat and Dominik, 2010) [8]; El-bassiony et al., 2018) [9].

The study area is located in the Herodotus basin offshore West Egypt (Fig.2). It includes many structural domains, from southwest to northeast; narrow shelf zone; trending transform margin; Herodotus Basin; Herodotus Fold Belt, and Matruh canyon to the east (Baer et al., 2017) [10]. The shelf area is relatively narrow and it extends to the onshore discovery belt, where the Alam El Bueib (Lower Cretaceous) and Khatatba (Jurassic) reservoirs are found.

The Herodotus Basin is a Tertiary sag area subsequently formed during the opening of the Neo-Tethys (Mid-Jurassic to Early Cretaceous times), where the Messinian Salt covered almost the entire area.

The Herodotus fold belt is linked with the Mediterranean Ridge. The Messinian Salt is folded due to tectonic compression and gravity-driven deformation. The salt-related anticlinal structures of the Pliocene sequence could form structural traps.

The Matruh Canyon is Early Cretaceous rift basin trending to the north-north-east and was inverted in the Late Cretaceous. The stratigraphy of the Matruh basin is related to the onshore well datasets (Tari et al., 2012 [11]; Barakat et al., 2019 [12]).

The study area covers several structures with a variant thickness of sediments from shallow to deep data (100 to 3000 m) in addition to the complex water bottom (Barakat,2010) [13]. The seismic processing of such data is challenging and needs the state of art in order to produce a high-resolution data quality (Abdullah et al.,2021) [14].

## Theoretical Background

When the marine sources (Air gun) release the high pressure into the seawater, an air bubble is generated and rapidly expands in the seawater. The bubbles are continuing repeatedly until all the energy is dissipated and breaks at the sea surface (Landrø et al., 2018) [15].

The release bubbles act as an additional acoustic pulse, the released pulse shape is the same as air guns which are used in the same survey in terms of amplitude and periodicity which is called source signature (Sagrang et al., 2016) [16].

The source signature can be obtained directly from the recorded Far-Field wavelet or model using source parameters of the acquired survey or using extracted wavelet from the recorded data (Hobbs and Jakubowicz, 2000) [17].

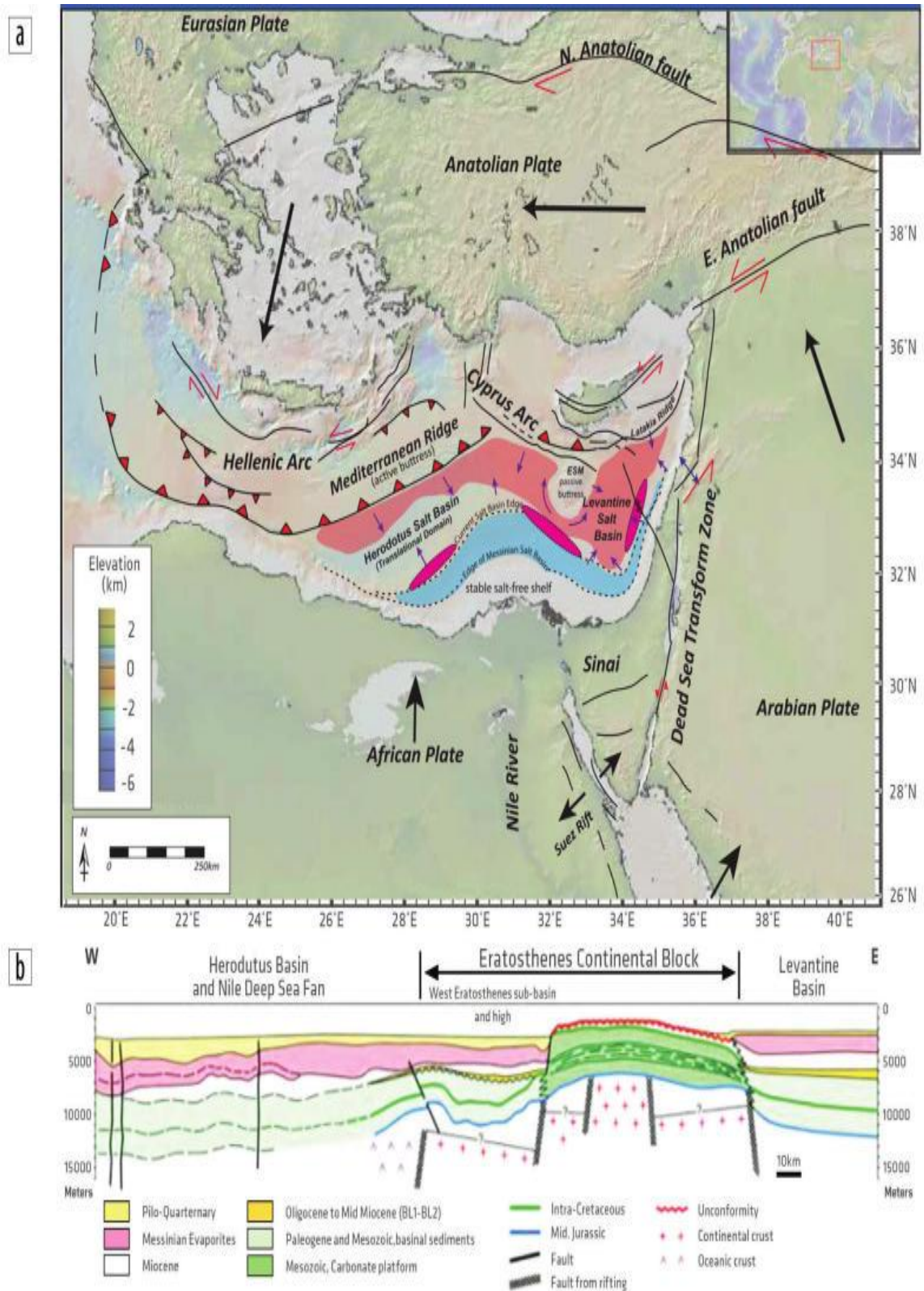


**Figure 1** Eastern Mediterranean (a) structural map (b) East-west stratigraphic sequence (El-Bassiony et al., 2018).

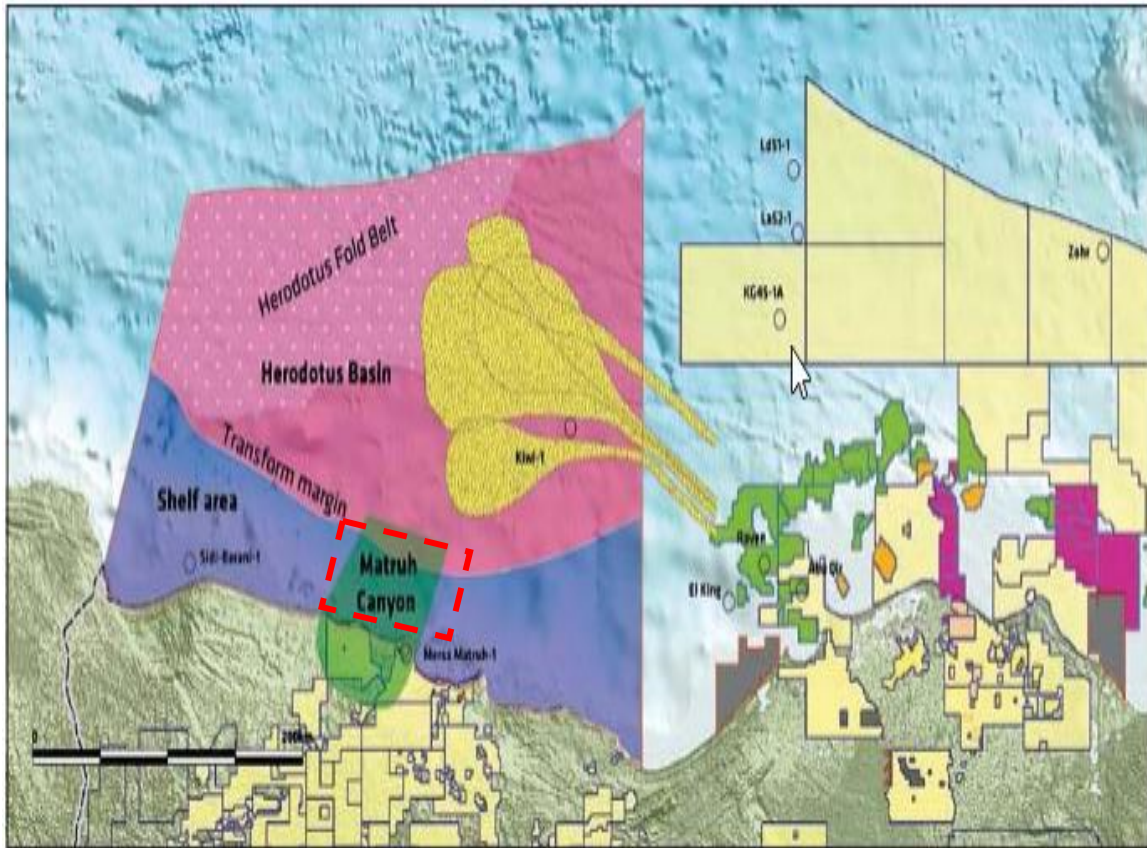


**Figure 2** The study area outlined in red , covers many different geological domains (Baer et al., 2017).

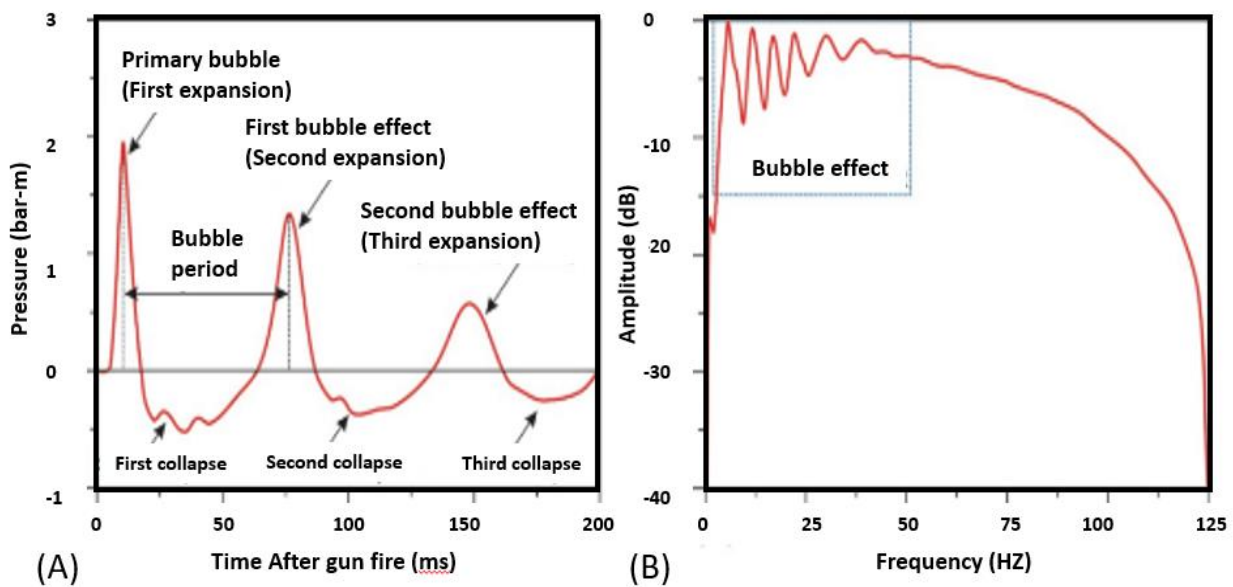


**Figure 3** (A) Typical Far-field signature, (B) amplitude Spectrum of the far field signature fired at 6m depth (after Derman 2018).

The recorded wavefield can be defined as the convolution of several independent components. In order to recover the earth impulse response, the effect of the seismic acquisition needs to be removed from the data during processing. The De-signature process aims to eliminate the undesirable components of the recorded data including the bubble effect and the Source response.

The bubble pulse generates a low-frequency peak on the amplitude spectrum of seismic data (Fig.3). The frequency is at 8–10 Hz with a harmonics series expanding up to at least 30 Hz (Dondurur, 2018) [18].

Several processing algorithms make the recorded seismic signal be expressed as a convolution of the emitted wavelet and the earth's impulse response.

$$y(t) = w(t) * f(t) \quad (1)$$

Where:

$y(t)$  = recorded signal;

$w(t)$  = emitted wavelet; and

$f(t)$  = impulse response required.

Theoretically, to remove the source signature, the design inverse filters for the signature wavelet in current data. The Wiener filter approach allows conversion from the input wavelet to any desired output wavelet (Breistøl, 2015) [19].

$$\begin{pmatrix} r_0 & r_1 & r_2 & \cdots & r_{n-1} \\ r_1 & r_0 & r_1 & \cdots & r_{n-2} \\ r_2 & r_1 & r_0 & \cdots & r_{n-3} \\ \vdots & \vdots & \vdots & \ddots & \vdots \\ r_{n-1} & r_{n-2} & r_{n-3} & \cdots & r_0 \end{pmatrix} \begin{pmatrix} a_0 \\ a_1 \\ a_2 \\ \vdots \\ a_{n-1} \end{pmatrix} = \begin{pmatrix} g_0 \\ g_1 \\ g_2 \\ \vdots \\ g_{n-1} \end{pmatrix} \quad (2)$$

Where:

$r$  = auto correlation of the input wavelet

$a$  = filter coefficient

$g$  = cross-correlation of the desired output and the input wavelet.

The Wiener equation can be applied for filter design in a wide range. In this work, a Wiener De-signature filter was designed using the average recorded Far-Field signature as an input and reshaping it to the zero-phase equivalent of the desired output wavelet.

## Materials and Methods

The input average recorded the Far-Field signature from the recent 3D acquisition survey from offshore Egypt, the Mediterranean Sea, and the Near Channel data from the acquired survey after the De-ghosting stage. Source parameters are as follows, source type Bolt 1900 LLXT, number of sources 3, gun pressure 2000 psi, volume 3280 cu in, source separation 25 m, number of sub-arrays 2 per source, sub-array

separation 8 m, source array length 14 m, Source depth 7 m and Shot point interval 16.667 m.

Nucleus plus<sup>®</sup> software was used in the design of the De-signature filter. PGS software was used for the application of the designed De-signature filter.

To design the De-signature filter, the following steps were used:

Average the recorded Far-Field signature (Input Wavelet) is shown in Fig.4.

Determine the period of the bubbles from the amplitude term.

Generate the combined new reshaping amplitude term and new zero phase equivalent term (Desired output wavelet) in Figure 5.

Use the Wiener filter approach to design the output De-signature filter (operand is the input Average recorded Far-Field signature Wavelet and the operator is the Desired output wavelet).

The output 1D filter is the De-signature filter which is then applied to the marine seismic data to get rid of the bubble effect and convert the data into zero phasing data. (Fig.6).

The output wavelet after the application of the De-signature filter is zero phase and free from the bubble effect (Fig.7).

## Results and Discussion

The application of the derived De-signature filter using the proposed workflow on the input average Far-Field wavelet shows a good impact in terms of attenuating the bubble effect with a stable amplitude spectrum and converts the wavelet into zero phase without obvious artifacts.

On the other hand, the application of the derived De-signature filter on the seismic data recorded in complex water bottom from the Mediterranean Sea shows a good result in terms of removing the bubble energy and zero phasing the data with stable amplitude spectrum, as demonstrated in (Fig.8A) includes the Near Chan display before the application of the derived De-signature filter using the proposed workflow.

It clearly shows the oscillation of the bubbles effect on the recorded seismic data reduces the subsurface imaging resolution, (Fig.8B) is the autocorrelation display for the same Near Chan. The autocorrelation aims to demonstrate the similarity of a time series of the trace with itself.

This reflects periodical components embedded within the data due to the periodical repetition for the bubble oscillation.

Figure (9A) illustrates the Near Chan display after using the proposal workflow to apply the derived De-signature filter. It demonstrates the attenuation of bubble oscillation and increases the resolution of subsurface imaging without obvious artefacts. Figure (9B) shows the autocorrelation of the Near Chan after applying the derived De-signature filter, which results

in good attenuation of the bubble oscillations with no obvious residual bubbles. Figure (10) shows the amplitude spectrum for a design window before and after the application of the derived De-signature filter. This clearly shows that the high amplitude and low frequency bubbles are nicely removed with stable broadband of amplitude spectrum.

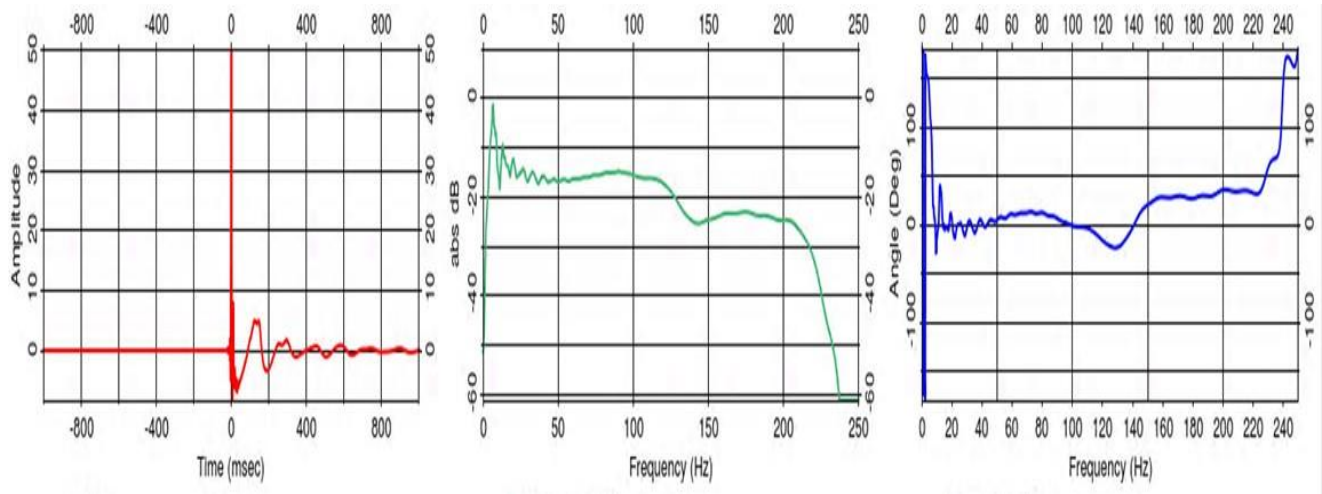


Figure 4 Input Far-Field signature.

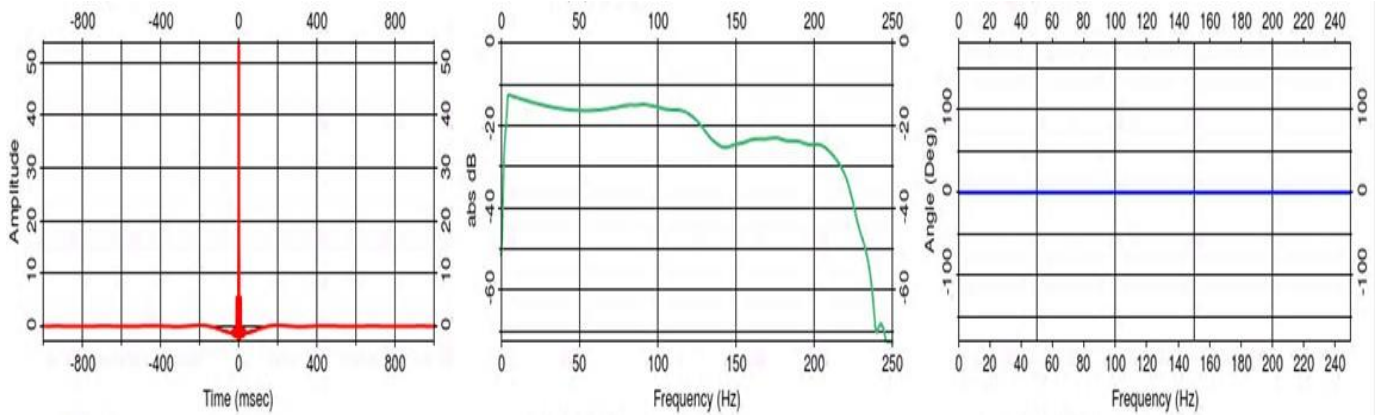


Figure 5 Desired wavelet output including the amplitude reshaping term and zero phase term.

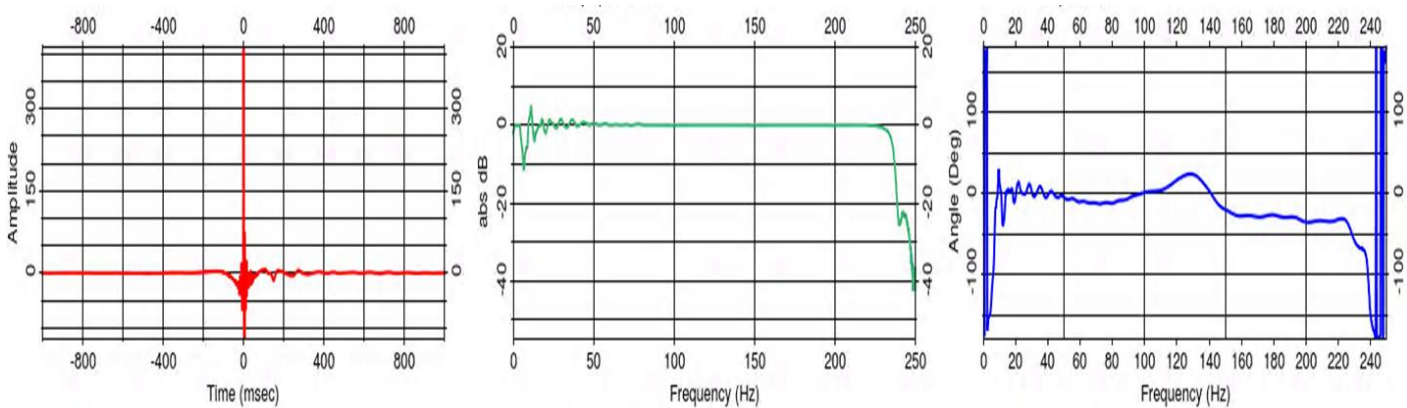


Figure 6 Output De-signature filter.

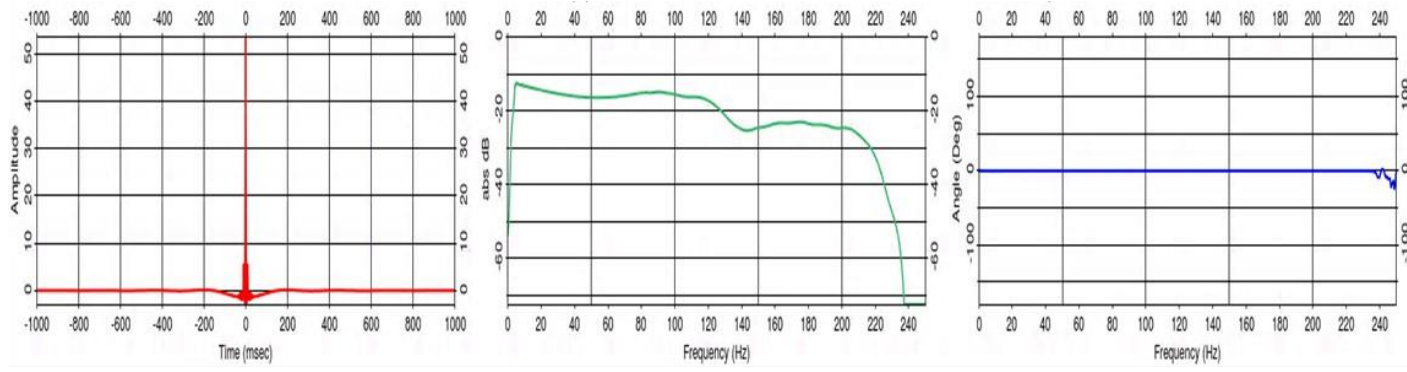


Figure 7 Output wavelet after application of the De-signature filter.

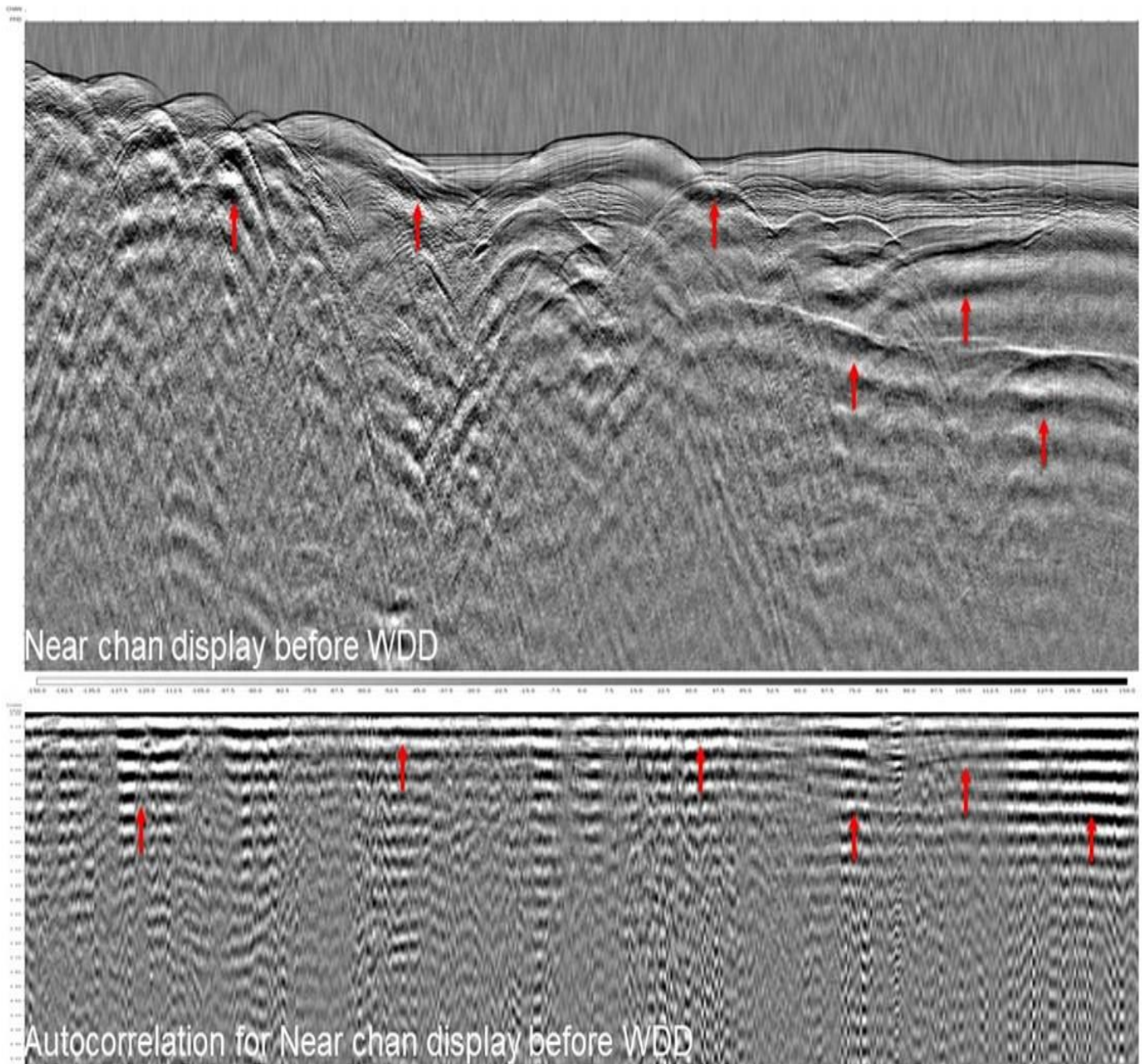


Figure 8 (A) Near Chan display, (B)Autocorrelation for the Near chan before De-signature application using WDD workflow

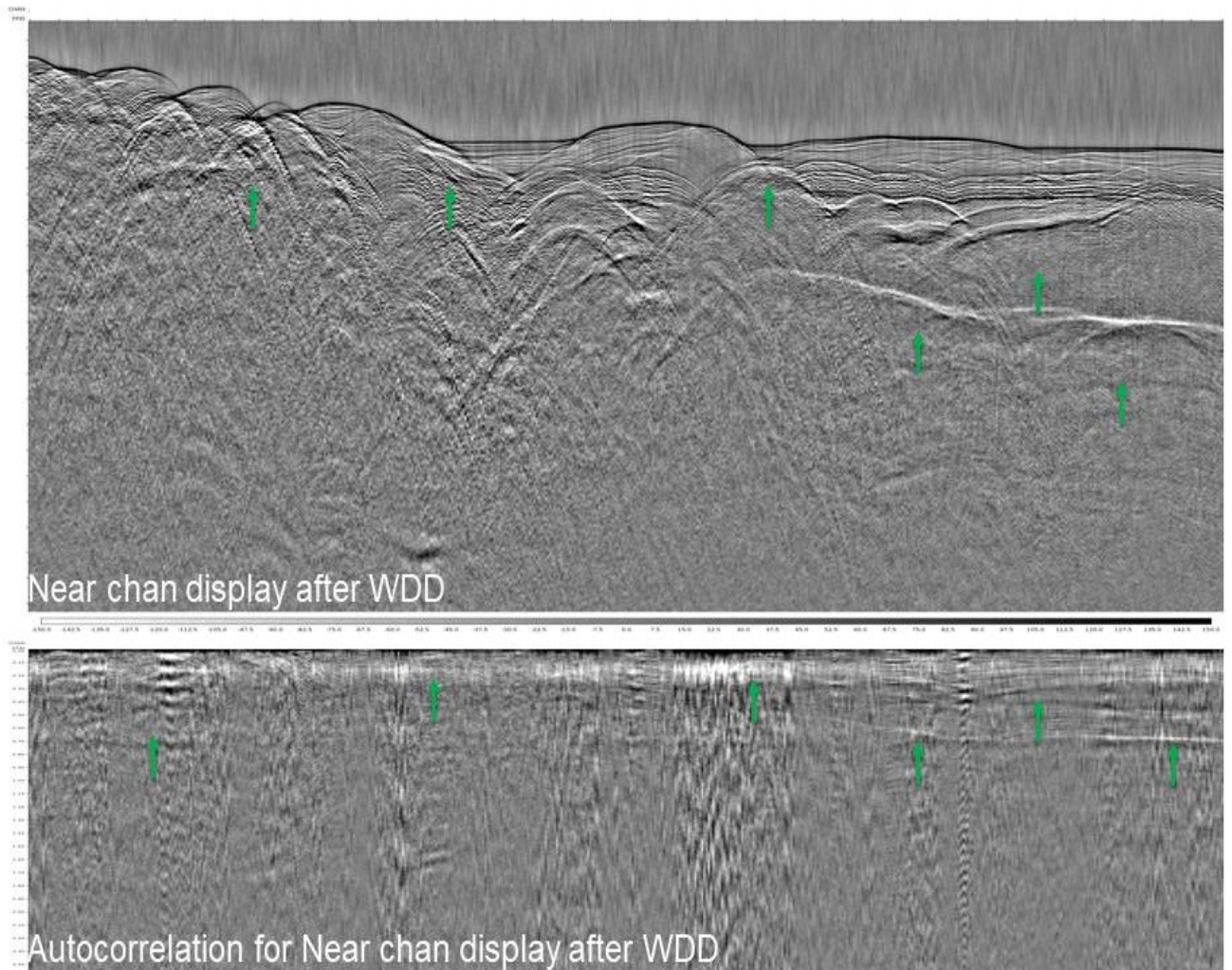


Fig.9. (A) Near Chan display, (B) Autocorrelation for the Near chan after De-signature application using WDD workflow.

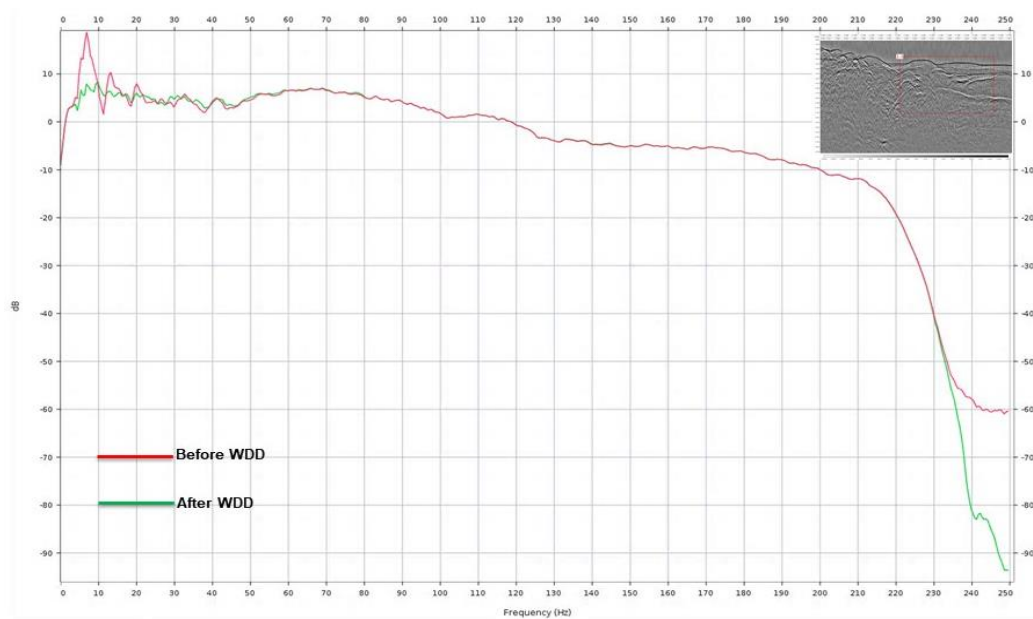


Fig.10. Amplitude Spectrum before and after After De-signature application using WDD workflow.

Figure (11) represents the decomposition of the recorded seismic data into frequency panels (Octave panels) before the application of the derived De-signature filter. It shows that the low-frequency bubbles are observed from 0 to 32 HZ and reduce the resolution of the low-frequency data.

Figure (12) is the same Octave panels after application of the derived De-signature filter which shows a clear attenuation of the bubbles oscillation for the recorded seismic data as well as good continuity of the seismic events due to the inclusion of the zero-phase term to the De-signature filter.

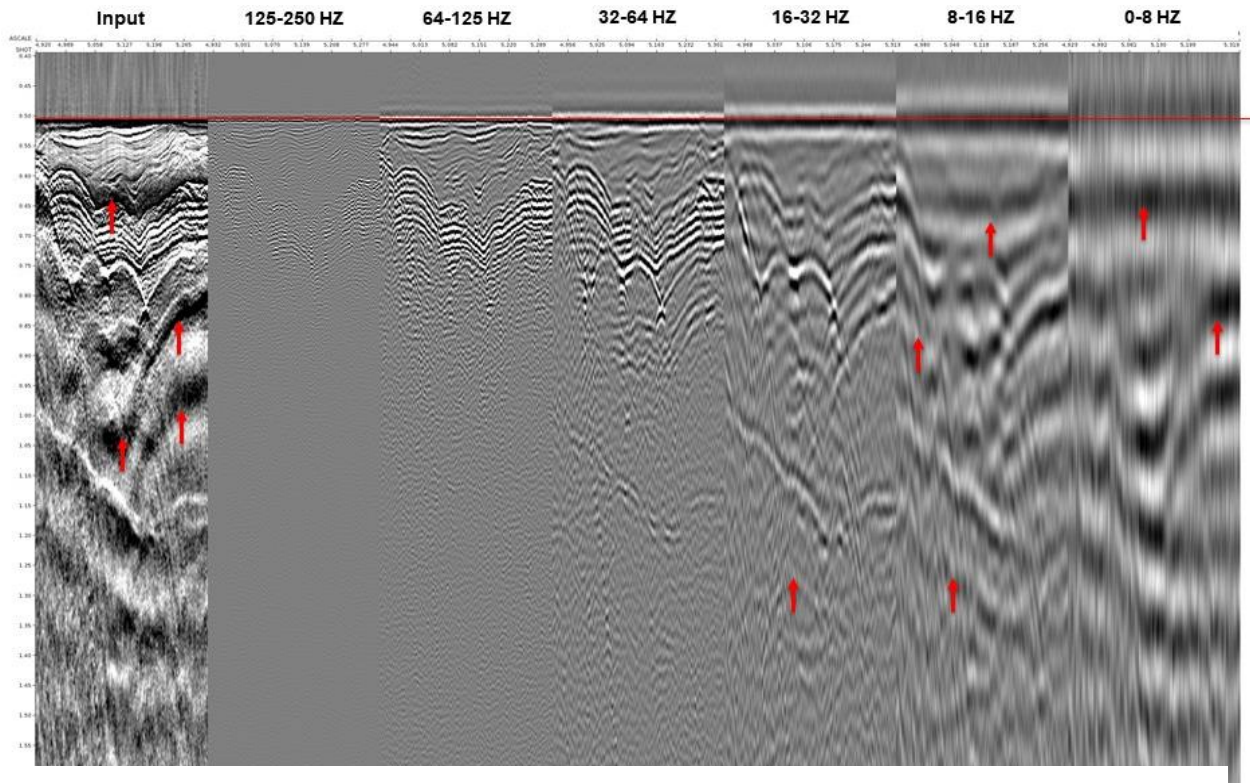


Fig.11.Frequency panel displays for the Near chan before De-signature application.

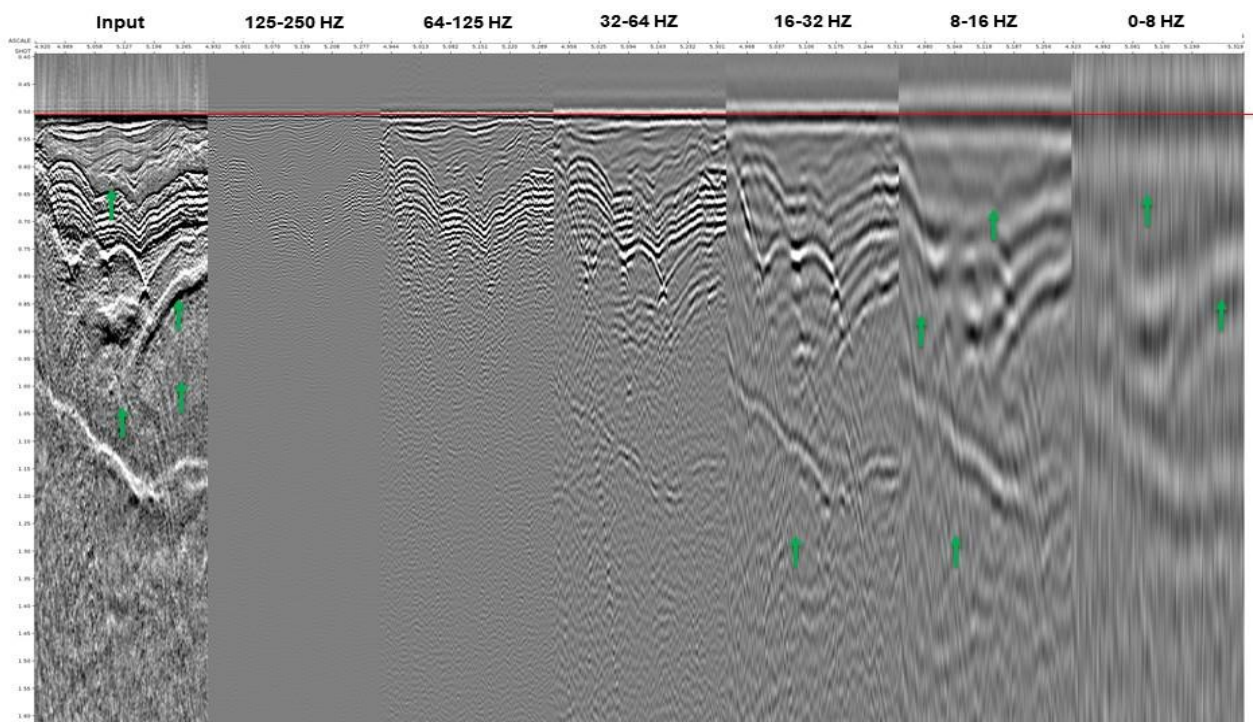


Fig.12.Frequency panel displays for the Near chan after De-signature application.

## Conclusions

The low-frequency residual bubbles in marine seismic data poses a significant challenge in data processing, particularly in case of complex water bottom areas. It is now possible to completely remove the bubble effect from data using robust and consistent acquisition parameters, in addition to the application of the presented optimum proposed workflow. This was demonstrated in this work by using the proposed workflow on newly acquired data at the study area in the Mediterranean Sea, offshore Egypt. The workflow has been tested in vintage areas, but residual bubbles were observed due to the instability of the source parameters or due to inaccurate reshaping parameters for the input wavelet to the workflow which needs some test to get the optimum parameters.

The main benefit of the Wavelet dependent De-signature workflow are,

- The proposed workflow is depending on only one input wavelet to drive the De-signature filter.
- The reshaping and zero phase equivalents were derived from the input wavelet, with no need for additional desire output wavelet.
- The frequency band of the amplitude reshaping is determined directly from the input wavelet.
- The full bandwidth is preserved, no predictive deconvolution is employed.
- The input wavelet could be the recorded Far-Field or Near field signature or modelled Far-Field signature or extracted wavelet from the seismic data.
- The optimization of the amplitude reshaping is the main factor to output a robust De-signature filter.

Finally, the combination of the stable Far-Field signature and reshaping parameters have complemented each other to get a stable De-signature filter.

## Funding sources

This research received no external funding.

## Conflicts of interest

There are no conflicts to declare.

## Acknowledgements

The authors wish to thank PGS for their support and Joshua May, Charles Zeltser, and Mokhtar Raafat for providing the raw seismic data, Special thanks to the editor-in-Chief, and the reviewers for the valuable discussions and effective reviews. Moreover, our deep appreciations to Jyoti kumar geophysical support manager at Petroleum Geo-Service (PGS) for revising the language of the manuscript.

## References

- [1] Y. Belhassen, I. Souza, R. Pereira, E. Tomaz, D. Carotti, D. Donno, I. Zoukaneri, 3D designature and deghosting in complex geology: application to Brazilian Equatorial margin data, 15<sup>th</sup> International Congress of the Brazilian Geophysical (2017).
- [2] J. C. Egbai, E. Atakpo, C.O. Aigbogun, Predictive deconvolution in seismic data processing in Atala prospect of rivers State, Nigeria, *Adv. Appl. Sci. Res.*, (2012) 3(1):520-529.
- [3] S. Goffredo and Z. Dubinsky, *The Mediterranean Sea: Its history and present challenges*, 2014, page 3.
- [4] S. Gradmann, C. Hübscher, Z. Ben-Avraham, D. Gajewski, G. Netzeband, Salt tectonics off northern Israel: Marine and Petroleum Geology, 22, (2005) no. 5, 597–611, <https://doi.org/10.1016/j.marpetgeo.02.001>.
- [5] Z. Ben-Avraham, A. Ginzburg, J. Makris, L. Eppelbaum, Crustal structure of the Levant Basin, eastern Mediterranean: Tectonophysics, 346, (2002) no. 1-2, 23–43, [https://doi.org/10.1016/S0040-1951\(01\)00226-8](https://doi.org/10.1016/S0040-1951(01)00226-8).
- [6] B. Voogd, C. Truffert, Two-ship deep seismic soundings in the basins of the eastern Mediterranean Sea (Pasiphae cruise): Geophysical Journal International, 109, (1992) no. 3, 536–552, <https://doi.org/10.1111/j.1365-246X.1992.tb00116.x>
- [7] Z. Garfunkel, Constrains on the origin and history of the Eastern Mediterranean Basin: Tectonophysics, 298, (1998) no. 1-3, 5–35, [https://doi.org/10.1016/S0040-1951\(98\)00176-0](https://doi.org/10.1016/S0040-1951(98)00176-0).
- [8] M. Kh. Barakat, W. Dominik, Seismic studies on the messinian rocks in the onshore Nile Delta, Egypt. 72<sup>nd</sup> European Association of Geoscientists and Engineers Conference and Exhibition 2010: A New Spring for Geoscience. Incorporating SPE EUROPEC 2010, (2010) 7, pp. 5422–5426.
- [9] A. El-Bassiony, J. Kumar, T. Martin, Velocity model building in the major basins of the eastern Mediterranean Sea for imaging regional prospective. *The Leading Edge*, 37(7), (2018) 519–528. <https://doi.org/10.1190/tle37.070519.1>.
- [10] S. Baer, Ø. Lie, A. Al Morshedy, New Opportunities Offshore West Egypt GEO ExPro (2017) p.42-45.
- [11] G. Tari, H. Husseini, B. Novotny, K. Hannke, R. Kohazy, Play types of deep-water Matruh and Herodotus basins, NW Egypt Petroleum Geoscience (18), (2012) p.433-455.
- [12] M. Kh. Barakat, N. El-Gendy, M. El-Bastawesy, Structural modeling of the Alam El-Bueib Formation in the jade oil field, Western Desert, Egypt *J. Afr Earth Sci* 156:(2019)168–177.
- [13] M. Kh. Barakat, Modern geophysical techniques for constructing a 3D geological model on the Nile

- Delta, Egypt. PhD Dissertation: Technische Universität Berlin, 158. (2010).
- [14] E. Abdullah, N. Al-Areeq, M. Elmahdy, M. Barakat, A new insight into the structural architecture of Sharyoof field, Say'un–Masilah basin, Yemen Arabian Journal of Geosciences (2021) 14:1977. doi.org/10.1007/s12517-021-08299-2
- [15] M. Landrø, L. Amundsen, Introduction to exploration geophysics with recent advances. Bivrost Geo. 341 pages (2018). ISBN: 978-82-303.
- [16] C. SAGRANT, W. Richard, R. Darren, Improving the interpretability of air-gun seismic reflection data using deterministic filters, geophysics, vol. 76. (2016).
- [17] R. Hobbs, H. Jakubowicz, Marine source signature measurement using a reference seismic source: 70<sup>th</sup> Annual International Meeting, SEG, Expanded Abstracts, 57–6. (2000).
- [18] D. Dondurur, Acquisition and processing of Marine seismic data, Airgunarray, p 62. (2018).
- [19] A. Breistøl, Broadband processing of conventional 3D seismic data for near surface geohazard investigation: A North Sea case study. (M.Sc. Thesis) Norwegian University of Science and Technology. 87 pp. (2015).